

*ARMY RESEARCH LABORATORY*



# 3-D Parachute Descent Analysis Using Coupled Computational Fluid Dynamic and Structural Codes

Jubaraj Sahu  
Gene R. Cooper  
Richard J. Benney

ARL-TR-1435

SEPTEMBER 1997

DTIC QUALITY INSPECTED 2

19971017 128

The findings in this report are not to be construed as an official Department of the Army position  
unless so designated by other authorized documents.

Citation of manufacturer's or trade names does not constitute an official endorsement or approval of  
the use thereof.

Destroy this report when it is no longer needed. Do not return it to the originator.

# **Army Research Laboratory**

Aberdeen Proving Ground, MD 21005-5066

---

---

ARL-TR-1435

September 1997

---

## **3-D Parachute Descent Analysis Using Coupled Computational Fluid Dynamic and Structural Codes**

Jubaraj Sahu

Gene R. Cooper

Weapons & Materials Research Directorate, ARL

Richard J. Benney

Natick Research, Development, and Engineering Center

U.S. Army Soldier Systems Command

---

Approved for public release; distribution is unlimited.

---

---

---

## Abstract

---

A computational tool that models the terminal descent characteristics of a single or a cluster of parachutes is a technology that is needed by parachute designers and engineers. As part of a technology program annex (TPA), a joint effort between the U.S. Army Natick Research, Development, and Engineering Center (NRDEC) and the U.S. Army Research Laboratory (ARL) to develop this computational tool is now under way. As a first effort, attempts are being made to analyze both two-dimensional (2-D) and three-dimensional (3-D) flow fields around a parachute using a coupling procedure in which the fluid dynamics are coupled to 2-D and 3-D structural dynamic (SD) codes. This effort uses computational fluid dynamic (CFD) codes to calculate a pressure field, which is then used as an input load for the SD code. Specifically, this report presents the methods and results of the flow field plus the structural characteristics of a single axisymmetric parachute and a 3-D gore configuration for the terminal descent velocity. Computed results have been obtained using the payload weight and unstretched constructed geometry of the canopies as input. Significant progress has been made in determining the terminal descent flow field along with the terminal shape of the parachute. A discussion of the fluid and structural dynamics codes, coupling procedure, and the associated technical difficulties is presented. Examples of the codes' current capabilities are shown.

## TABLE OF CONTENTS

	<u>Page</u>
LIST OF FIGURES .....	v
1. INTRODUCTION .....	1
2. SOLUTION TECHNIQUE .....	2
2.1 Computational Fluid Dynamics Model .....	2
2.2 Current Structural Dynamics Model .....	3
2.3 Coupling Procedure .....	4
3. MODEL GEOMETRY AND COMPUTATIONAL GRID .....	5
4. RESULTS .....	7
5. CONCLUDING REMARKS .....	14
6. REFERENCES .....	17
DISTRIBUTION LIST .....	19
REPORT DOCUMENTATION PAGE .....	23

**INTENTIONALLY LEFT BLANK**

## LIST OF FIGURES

<u>Figure</u>		<u>Page</u>
1. Computational Grid for Axisymmetric Parachute . . . . .	6	
2. An Expanded View of the Grid Near the Parachute . . . . .	6	
3. Velocity Vectors for Axisymmetric Parachute, $\alpha = 0^\circ$ . . . . .	7	
4. Comparison of Pressure Distributions (axisymmetric case) . . . . .	8	
5. Single Gore Surface Grid . . . . .	9	
6. 3-D Computational Grid for Gore . . . . .	10	
7. Pressure Contours for Gore, $\alpha = 0^\circ$ . . . . .	10	
8. Computed Surface Pressure for Gore, $\alpha = 0^\circ$ , (inner and outer) . . . . .	11	
9. Comparison of Gore Shapes for Different Coupling Iterations, $\alpha = 0^\circ$ . . . . .	12	
10. 3-D Gore Pressure Distributions at Different Circumferential Locations . . . . .	13	
11. Comparison of Pressure Distributions (3-D gore, inner surface) . . . . .	14	
12. Comparison of Pressure Distributions (3-D gore, outer surface) . . . . .	14	

INTENTIONALLY LEFT BLANK

## 3-D PARACHUTE DESCENT ANALYSIS USING COUPLED COMPUTATIONAL FLUID DYNAMIC AND STRUCTURAL CODES

### 1. INTRODUCTION

Parachutes have been an interest to man for more than 2,000 years.<sup>1</sup> A brief but good review of the history of parachutes is presented in Cockrell (1987),<sup>2</sup> Knacke (1987),<sup>3</sup> and the U.S. Air Force 1978 and 1963 Parachute Design Guides.<sup>4,5</sup> The consideration of parachutes as high-performance aerodynamic decelerators did not take place until the middle of this century. One of the features of parachutes that is being studied here is the fluid flow field around one or more parachutes being used as decelerators for heavy payloads dropped from in-flight aircraft. In particular, this work investigates the coupling of the flow field around non-ribbon parachutes with the dynamic structure of the parachutes themselves.

The flow around parachutes has been studied by many investigators<sup>2,6,7</sup> using analytical methods for predicting canopy pressure distributions. Cockrell (1987)<sup>2</sup> presents a summary of potential flow solutions describing steady state canopy pressure fields, and Reference 1 describes closed form analytical solutions for the velocity potential around spherical cups. These studies have been extended by Klimas (1972),<sup>7</sup> who considered placing a vortex sheet to coincide with the location of a real canopy. He used an axisymmetric Stoke's stream function to model viscous and permeable material effects. The theoretical predictions gave only fair numerical results, but the internal flow behavior was reasonably good.

Researchers have continued to study the flow around parachutes using numerical methods to solve the governing equations. A two-dimensional computational fluid dynamic (CFD) code has been used by the U.S. Army Natick Research, Development, and Engineering Center (NRDEC). NRDEC has applied this code to flow problems that have axial symmetry and have calculated the flow and pressure fields around parachutes. One limitation of using a two-dimensional (2-D) code is that the parachutes of interest are usually not axisymmetric. Therefore, this report is going to investigate the three-dimensional (3-D) properties of flows around parachutes. The pressure distributions calculated on the top side and underneath the parachutes are then used to couple the fluid dynamics to the structure codes used to model the structural properties of the parachute itself.

The total drag of parachutes in a cluster has been shown experimentally to be less than the sum of the drags of the individual canopies. The ability to predict the flow field characteristics, terminal descent positions/shapes, and the drag on clusters of parachutes is needed to assist in

the development of improved parachute cluster design and should allow for optimization studies to be performed numerically. A joint effort between NRDEC and the U.S. Army Research Laboratory (ARL) to develop this computational tool has begun with modeling flow about parachutes in 3-D. This effort is using 3-D CFD codes in conjunction with 3-D structural dynamics (SD) codes.

The aerodynamic characteristics associated with a single or cluster of parachutes in the terminal descent phase are extremely complex to model. The complexity arises largely from the fact that the flow field depends on the canopy shape, which itself depends on the flow field. A correct model must include the coupled behavior of the parachute system's structural dynamics with the aerodynamics of the surrounding flow field. The coupled model is being developed to yield the terminal descent characteristics of single or clustered parachutes including velocity, shape, drag, pressure distribution, and the other flow field characteristics.

As a starting point, the terminal descent characteristics of a half-scale C-9 solid flat circular parachute are determined. The goal for this step is to predict the parachute's terminal descent shape, velocity, pressure field, velocity field, etc., when the payload weight and unstretched constructed geometry of the canopy are given as input. This 3-D capability is needed to allow design engineers to optimize a single parachute design (for terminal descent characteristics) on a computer. The effect on the parachute's terminal descent characteristics because of modifications of a gore shape, suspension line length, etc., can be investigated without having to manufacture prototypes and perform multiple drop tests. The 3-D CFD/SD capability being developed will ultimately be applied to the parachute cluster problem to investigate the flow field surrounding various U.S. Army clustered parachute configurations.

This report describes the progress made in the development of the CFD and SD models. The approach used to couple the two codes is also described. Examples of the codes' current capabilities are presented.

## 2. SOLUTION TECHNIQUE

### 2.1 Computational Fluid Dynamics Model

The computational method used in the present analysis solves the incompressible Navier-Stokes equations in 3D (INS3D)<sup>8</sup> generalized coordinates for low-speed flows. This technique is based on the method of artificial compressibility and an upwind differencing scheme. The pseudo-compressibility algorithm couples the pressure and velocity fields at the same time level

and produces a hyperbolic system of equations. The upwind differencing leads to a more diagonal system and does not require a user-specified artificial dissipation. The viscous flux derivatives are computed using central differencing. This code is capable of computing both steady state and time accurate flow fields.

The governing equations are numerically represented and solved using a nonfactored Gauss-Seidal line-relaxation scheme. This maintains the stability and allows a large pseudo-time step to be taken to obtain steady state results. Details of the numerical method are given in Rogers, Wiltberger, and Kwak (1993)<sup>9</sup> and Kwak (1989).<sup>10</sup> To compute turbulent flows, a turbulence model must be specified. The present calculations use the one-equation turbulence model developed by Baldwin and Barth (1991).<sup>11</sup> In this model, a transport equation is solved for the turbulent Reynolds number. This equation is derived from a simplified form of the standard two-equation k- $\epsilon$  turbulence model. The one-equation model has the advantage that it does not require the turbulent length scale to be specified. It is solved using the same Gauss-Seidal-type line-relaxation scheme used to solve the mean flow equations.

## 2.2 Current Structural Model

The current structural model being used for this modeling effort is the CAnopy Loads Analysis (CALA) code.<sup>12</sup> The next generation for the structural half of the terminal descent model of round parachutes will be a three-dimensional membrane/cable finite element-based code.<sup>13</sup> CALA is a static code that predicts the steady state shape and stresses for round parachutes. CALA requires the parachute's dimensions and a steady state pressure distribution along a radial (meridional arc length) as input. A radial is defined as the continuation of a suspension line from the skirt along a meridional arc length to the apex of the canopy. The radial can also be visualized as the connection of two adjacent gores.

The pressure distribution across the surface of the canopy is supplied by the CFD code as a function of the 3-D deformed canopy shape. The CALA code assumptions transform the pressure distribution into nodal forces that are tangential and normal to the radial position. The CALA code assumes that the horizontal members (defined as the curved strip of a gore connecting two adjacent radials) of a gore form sections of circular arcs and that the pressure distribution is uniform along the horizontal members. The horizontal members lie in planes that are defined by the surface normal vectors from two adjacent radials comprising one gore. The CALA code defines the static force per unit radial length applied to a radial location. These force equations include the variable  $\psi$ , which is defined as the gore bulge angle.  $\psi$  is determined

iteratively for the current iteration's surface configuration based on the constructed gore shape. The forces include approximations of the hoop force contribution based on the gore geometry.

The CALA code reiterates the shape by assuming an initial guess for the vent line tension. The code outputs the canopy shape, stresses, gore bulge angles, total drag, etc. The radial shape is extracted from the output and used in a Formula Translator (FORTRAN) code with the CALA assumptions to generate a set of 3-D data representing the shape of a gore.

### 2.3 Coupling Procedure

At this time, the codes are being manually coupled. The results section that follows describes the current modeling capability. This section outlines the steps that are taken to model either single or clusters of parachutes as the model progresses over the next year. The process begins with the structural model, which requires the geometry of the canopy and suspension lines as input. A guessed surface pressure distribution is used by the structural code to determine a first guess deformed shape for the canopy or canopies.

If the parachute system is a single canopy, the shape determined is supplied to the CFD code as is. A CFD mesh is generated around the surface shape provided. The CFD code solves for the flow field characteristics with a prescribed in-flow velocity. The 3-D surface pressure distribution is extracted from the CFD results and fed into the structural code. The structural code is executed with the new surface pressure distribution and predicts a new deformed shape. The total vertical drag is calculated, based on using the shape and pressure distribution. The new shape is fed back to a grid generator program, and a mesh is generated. This new mesh is used in the CFD code, and computations are performed to obtain the steady state result with the same in-flow velocity. The process is continued manually until shape and pressure distribution converge. The solution may diverge for relatively poor initial guesses of pressure distribution, in which case, the process may involve a more elaborate coupling procedure.

To model a cluster of canopies, the predicted single parachute shape is rotated by an initial guessed angle about the confluence point. A CFD mesh can be created around the surface shape provided and can use symmetry boundary conditions that depend on the number of parachutes in the cluster. The CFD code solves for the flow field characteristics with a prescribed in-flow velocity along the vertical axis. The 3-D surface pressure distribution is extracted from the CFD results, and the net radial force on the canopy is determined. The canopy shape is then rotated in the direction that is consistent with the predicted net force. The new canopy grid location is supplied to the CFD code, a new mesh is created, and the resulting surface pressure distribution

is used to determine the direction and extent of rotation required to reach a force equilibrium in the “radial” direction. Rerunning the structural code with the new surface pressure distribution, once the radial forces have been reduced to near zero, is then performed and the process continued. The total vertical drag is predicted, based on the shape and pressure distribution of the single canopy multiplied by the total number of canopies being modeled in the cluster.

### 3. MODEL GEOMETRY AND COMPUTATIONAL GRID

The coupled model was used to determine the 3-D terminal descent characteristics of a half-scale C-9 canopy. The half-scale C-9 is a solid cloth, flat circular canopy composed of 28 gores. The constructed diameter is 14 feet, and suspension lines are 12 feet long. The half-scale C-9 canopy has been used in a variety of experiments and its opening behavior was predicted with an axisymmetric coupled model developed at Natick.<sup>14</sup> This canopy was studied with the manually coupled codes, and the terminal descent results are compared to the results obtained from previous studies at Natick.

To start, an axisymmetric parachute shape was modeled to gain confidence in the 3-D CFD code’s predictive capability of the flow field characteristics around parachute-like shapes. The terminal descent shape from the axisymmetric model (case 1 in reference 14) was used to define the grid. A computational mesh was generated around a quarter of the canopy to use symmetry boundary conditions for the axisymmetric test case. The surface grid along with a longitudinal cross section of the full grid is shown in Figure 1. The full grid consists of 48 points in the streamwise direction, 19 points in the circumferential direction, and 80 points in the normal direction away from the body surface. The grid points are clustered near the body surface for viscous turbulent flow computations. The outer, in-flow, and downstream boundaries are placed sufficiently away from the body surface that they do not interfere with the convergence and accuracy of the computed flow field results. The grid was obtained by the Eagleview<sup>15</sup> grid generation program using an algebraic method and elliptic smoothing procedure. An expanded view of the computational grid near the parachute body surface is shown in Figure 2. This figure shows the computational grid for both end planes in the circumferential direction. Also included is a shaded parachute body surface. It shows the grid clustering near the body surface more clearly for the outer part of the body surface and the skirt. The grid was obtained for a circumferential plane and then rotated around to obtain the full grid containing 19 planes in the circumferential direction.

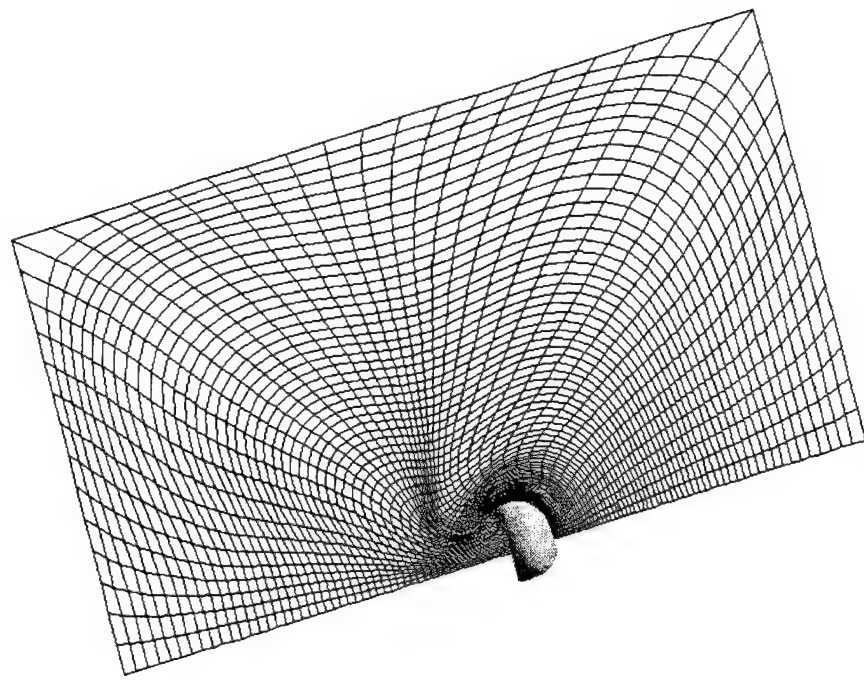


Figure 1. Computational Grid for Axisymmetric Parachute.

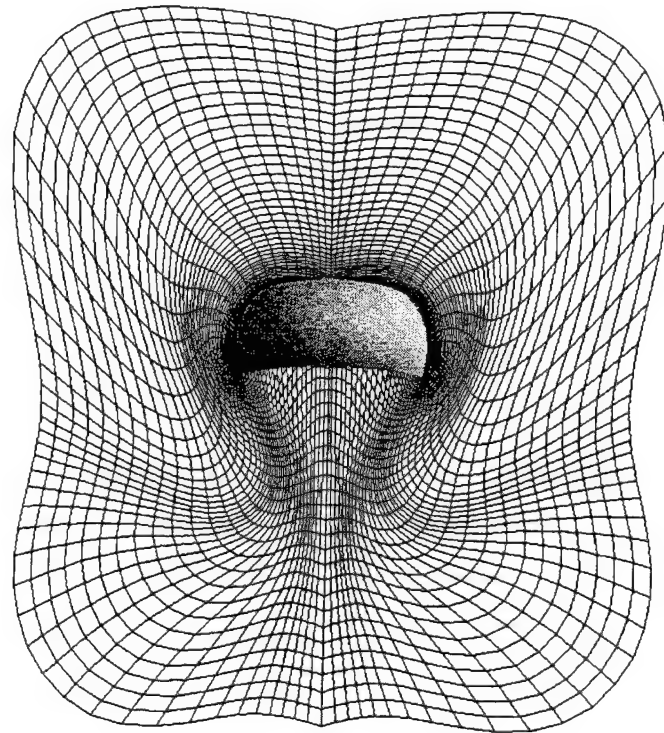


Figure 2. An Expanded View of the Grid Near the Parachute.

#### 4. RESULTS

The input velocity used is 18 feet per second, which was the terminal descent velocity determined from the axisymmetric model. All numerical computations were performed at this inflow velocity and at  $\alpha = 0^\circ$ . Results are now presented for the axisymmetric model. The computed results were obtained using the INS3D code. Figure 3 shows a velocity vectors field in the vicinity of the axisymmetric parachute shape. The incoming flow stagnates at the body surface, and a separated flow region is formed in front. It also shows flow separating at the skirt and then forming a large region of recirculatory flow behind the body. This separated flow region in the wake gives rise to lower surface pressure on the outer body surface.

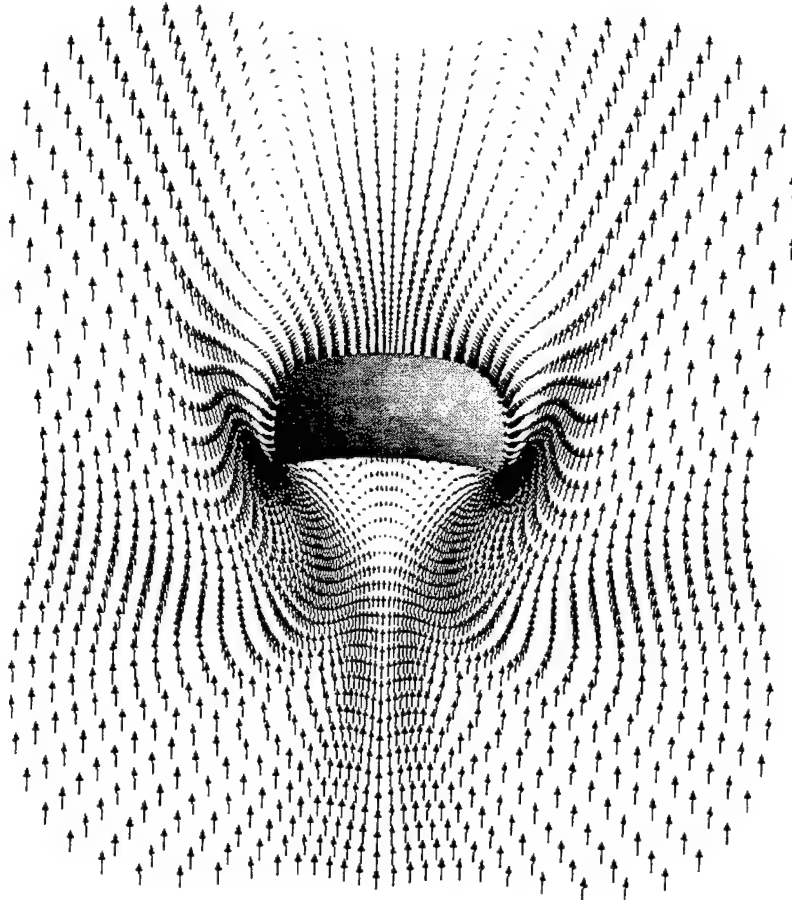


Figure 3. Velocity Vectors for Axisymmetric Parachute,  $\alpha = 0^\circ$ .

The pressure distribution on the inner and outer surfaces of the canopy from both codes is compared in Figure 4. In this figure, nondimensional pressure coefficient is plotted as a function of the meridional length. Here, the meridional length is the distance that is measured from the apex (vent) of the parachute to the outer section (skirt) along the canopy surface. The total meridional

length thus corresponds to half of the diameter of the parachute in the unstretched position (14 feet diameter). The computed pressure distributions obtained using the INS3D code are compared with the previous computed pressure distributions using a 2-D code. The two sets of computed results agree very well for both outer and inner surface pressures. The pressure distributions are very close, especially noting the fact that the axisymmetric coupled model had not completely damped at the time for which the shape was extracted. Small differences can be observed between these results near the skirt of the axisymmetric parachute. As expected, the inner surface pressure is quite uniform and is a lot higher than the predicted pressure on the outer surface. This gives rise to drag force, which is consistent with the payload for this parachute at this terminal velocity.

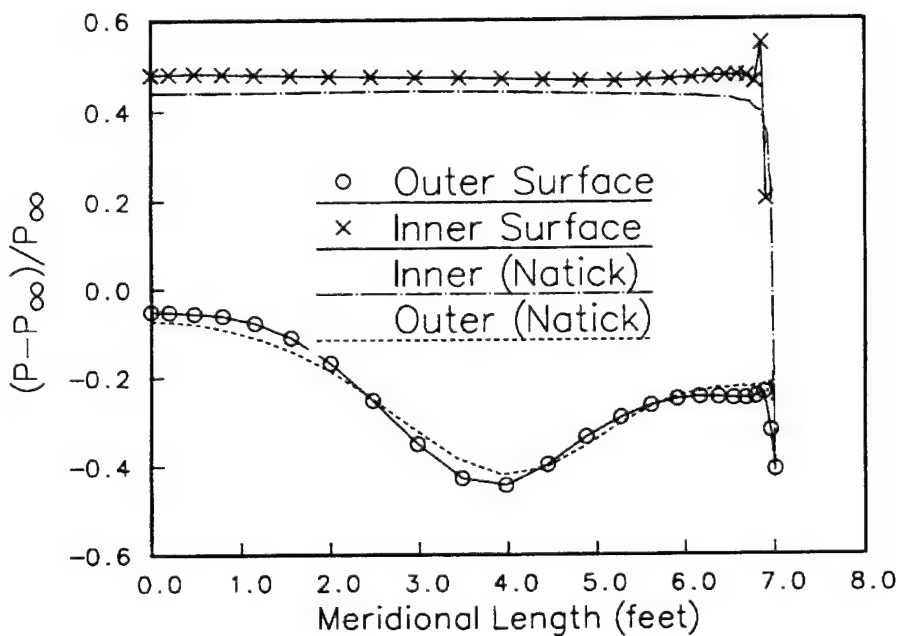


Figure 4. Comparison of Pressure Distributions (axisymmetric case).

The next step in this modeling effort involved extracting a 3-D grid of a single gore from the axisymmetric shape. This was done by applying the CALA assumptions of the gore shape to the radial node points. The axisymmetric shape is assumed to coincide with a radial. The 3-D gore surface was obtained using this procedure and further smoothed especially near the vent region to eliminate discontinuities in the surface definition. The smoothed surface grid is shown in Figure 5. This surface grid contains 24 grid points in the meridional direction and 22 points in the circumferential direction.

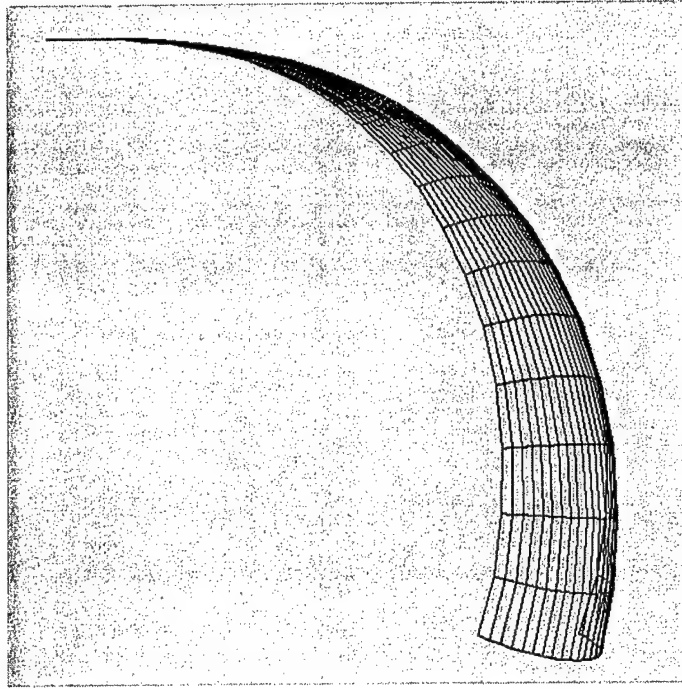


Figure 5. Single Gore Surface Grid.

This surface grid was used to generate a 3-D computational grid (see Figure 6) for the calculation of fluid flow over the gore configuration. The 3-D gore grid consists of  $53 \times 22 \times 84$  in the axial, normal, and circumferential directions, respectively. The section containing the gore surface was generated using an O-topology. Another section of the grid was obtained using rectangular mesh topology. Both grid components were generated algebraically<sup>15</sup> and then appended to form the full grid. The parachute gore surface is a part of an interior grid line, and thus, the no-slip boundary condition is applied along this interior boundary. For viscous flow computation, which is of interest here, the grid points are clustered near the parachute gore surface in the normal direction to resolve the flow gradients in the boundary layers.

Computed results have been obtained for the 3-D gore configuration and are now presented. Figure 7 shows the pressure contours for a circumferential end plane. For the incoming flow, the pressure is uniform (free-stream pressure). As the flow approaches the inner surface, pressure builds and forms a large region of high pressure in the vicinity of the inner surface. The pressure in the wake region is a low pressure region. Although there is some variation of pressure in the low pressure region, the outer surface pressure is a lot lower than the inner surface pressure. The flow expands around the skirt region of the gore, and sharp changes in the pressure field can be observed in going from the inner to the outer surface.

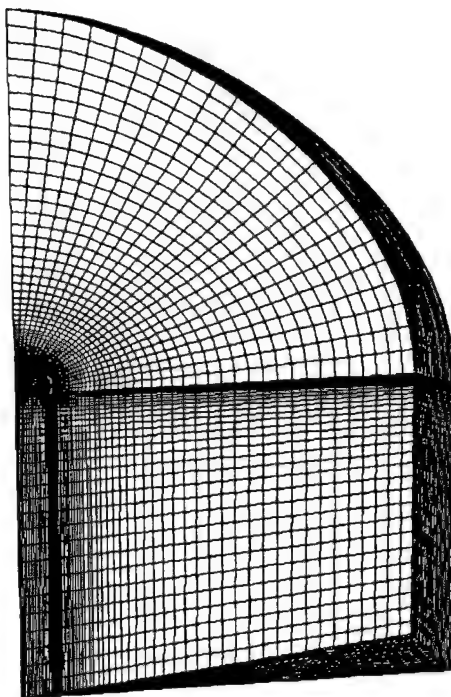


Figure 6. 3-D Computational Grid for Gore.

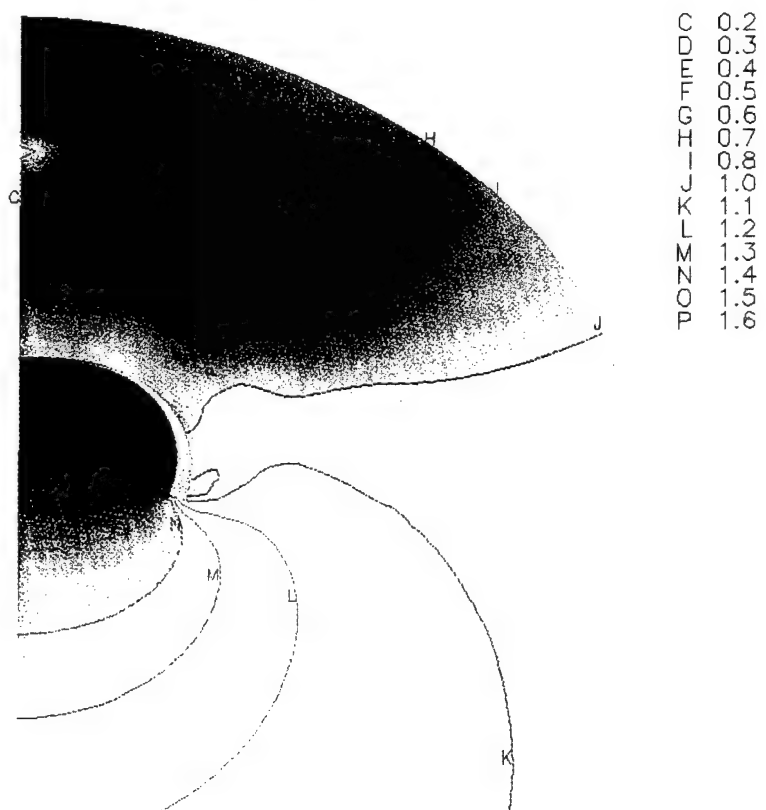


Figure 7. Pressure Contours for Gore,  $\alpha = 0^\circ$ .

The computed pressure map on the gore surface itself is shown in Figure 8 for both inner and outer surfaces. Although computations were performed on one gore shape because of symmetry, the canopy consists of 28 gores, which are all shown in this figure. Again, it shows high pressure on the inside surface, which is rather uniform except for the skirt region. The computed pressure on the outer surface is lower and is not as uniform.

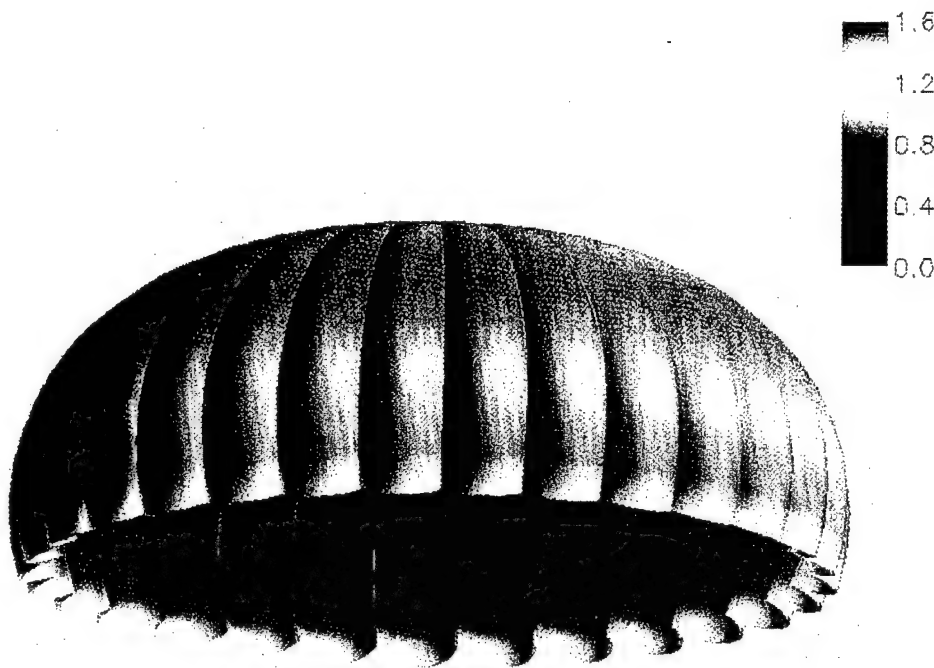


Figure 8. Computed Surface Pressure for Gore,  $\alpha = 0$ , (inner and outer).

The pressure distribution over the gore surface was used by the CALA code to predict a new shape for a gore. The pressure distribution required by CALA is assumed to be constant over the horizontal members of the gore. Therefore, the CFD predicted surface pressure distribution was averaged over the gore surface to obtain an average pressure distribution versus meridional arc length set of data. This was accomplished by averaging the surface pressure values at the radial location and the corresponding gore mid-point values. This pressure distribution was used as input by the CALA code which output the new predicted shape. The shape of the radial predicted to the CALA code was used as an input to a FORTRAN code that uses the CALA gore shape assumptions to generate a new 3-D gore grid. This new grid was used, computations were performed, and CFD results of the resulting flow field and pressure

distributions were obtained. This coupling procedure between the CFD and SD codes was repeated three times. The three different gore shapes that resulted from this analysis are shown in Figure 9. The change in the gore shape from the first iteration to the second was observed to be bigger than that from the second to the third iteration of this coupling procedure. The change between the shapes between the second and the third iteration was rather small, which indicates the near convergence of the body shape to its final terminal descent configuration.

The outer surface pressure distribution over the gore (first iteration) is shown as a function of meridional gore location in Figure 10. The total meridional length again corresponds to half diameter of the parachute in the unstretched position. The computed pressure distributions are obtained at different locations in the circumferential direction. The first plane in this figure refers to the edge of the gore whereas the half-plane corresponds to the mid-section (center) of the gore. The difference in the outer surface pressures is rather small over a large portion of the gore except near the skirt region. Although not shown here the same is true of the inner surface pressure distributions. For the subsequent figures on surface pressure comparisons, the 3-D gore surface pressure is used at the half-plane or the mid-section.

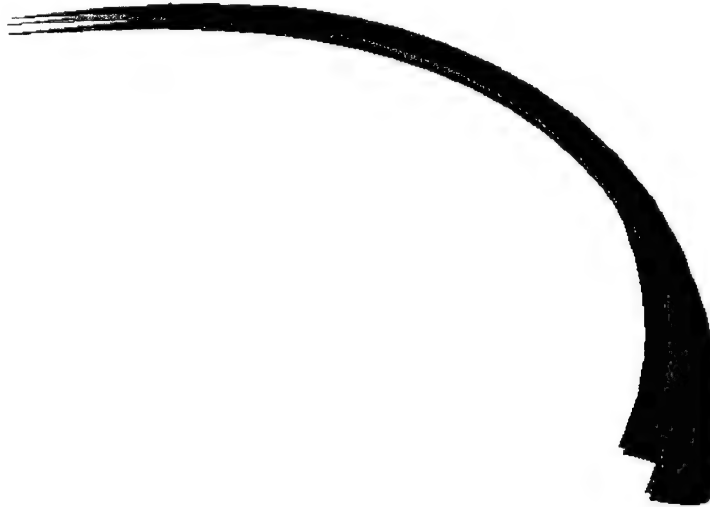


Figure 9. Comparison of Gore Shapes for Different Coupling Iterations,  $\alpha = 0$ .

The computed pressure distributions are all obtained using the INS3D code and are now compared between the different iterations of the coupling procedure described earlier. The inner surface pressure distribution over the 3-D gore is shown as a function of meridional gore location

in Figure 11. Also included in this figure is the computed pressure distribution for the axisymmetric parachute shape. The pressure distribution over the 3-D gore is nearly constant near the apex and deviates across the gore as the skirt is approached. This is expected because the shape is nearly axisymmetric near the apex and becomes less axisymmetric toward the skirt. The CFD code was run with the same in-flow velocity, and the 3-D parachute gore surface pressure distribution was extracted from the CFD results. The change in inner surface pressure is small between the different iterations or gore shapes and is especially small between the second and third iterations. The difference between the predicted pressure for the gore shapes and the axisymmetric configuration is larger, which indicates the necessity of 3-D modeling of the fluid and structural dynamics. Figure 12 shows the outer gore surface pressure comparisons at  $\alpha = 0^\circ$ . The three sets of gore shapes yield similar pressure distributions. The difference between the second and the third iteration again is smaller compared to that between the first and the second iteration. The pressure distributions for the different gore shapes do not show as large a variation in pressure as is observed for the axisymmetric parachute shape. The computed surface pressures for both 3-D gore and axisymmetric parachute agree rather well with each other only near the apex (vent). As expected, the 3-D effect is felt more near the skirt of the canopy. The pressure differential between the inner and the outer surface is what determines the drag force for these parachute shapes for a given terminal descent velocity.

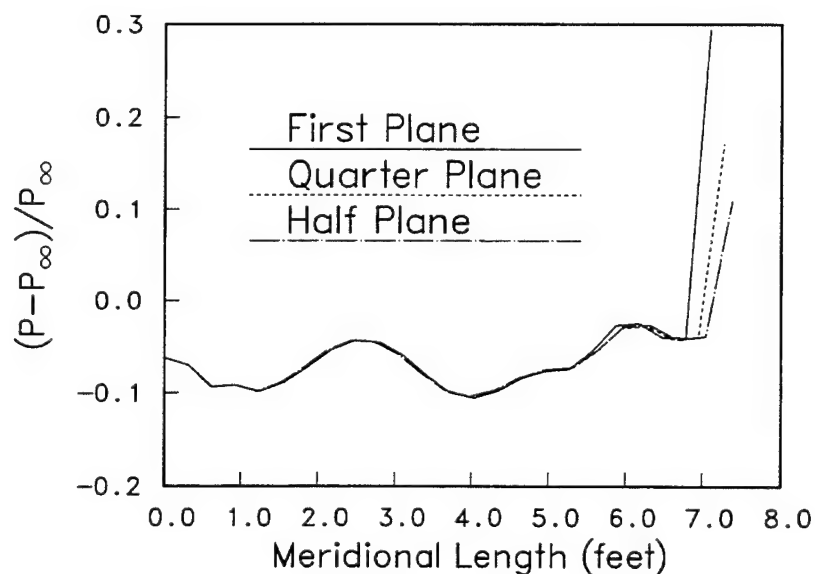


Figure 10. 3-D Gore Pressure Distributions at Different Circumferential Locations.

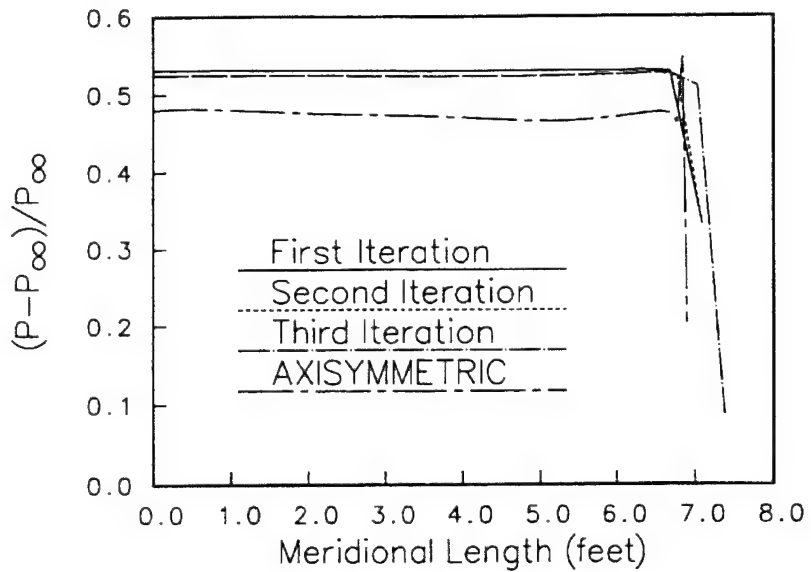


Figure 11. Comparison of Pressure Distributions (3-D gore, inner surface).

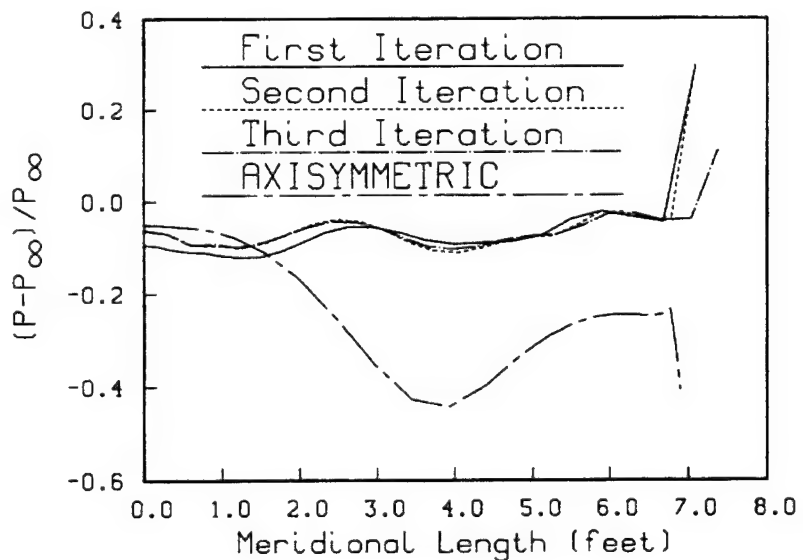


Figure 12. Comparison of Pressure Distributions (3-D gore, outer surface).

## 5. CONCLUDING REMARKS

The complexity of modeling parachute characteristics and phenomena in terminal descent and during the opening process stems from the coupling between the structural dynamics of the canopy, lines plus payload, and the aerodynamics of the surrounding fluid medium.

This report has described ongoing research being conducted at both NRDEC and ARL to predict the 3-D terminal descent characteristics of single and clusters of round parachutes. This involves the coupling of a 2-D and/or 3-D CFD code with 2-D and/or 3-D parachute structural codes. The solution to the coupled problem is expected to assist in the development of future U.S. Army airdrop systems and other round parachute systems. The capability of accurately predicting the behavior of parachute systems will significantly reduce the amount of testing currently required. The prediction of the terminal descent characteristics of a half-scale C-9 parachute has been demonstrated by manually coupling a 3-D CFD code to the CALA code. A 3-D membrane/cable finite element code will be used as the next generation structural model. Time will also be spent combining the two codes into a more user-friendly environment and enhancing the pre- and post-processing codes to shorten the turnaround time.

This report has presented the current status of the modeling effort and outlined the direction being pursued to address the complexity of the parachute characteristics and the associated flow fields. Future computational models are expected to provide better understanding of the physics that govern the parachute and flow field interaction. The codes will allow the user to examine the effect of vent size, vent location, varying suspension line lengths, etc.

INTENTIONALLY LEFT BLANK

## 6. REFERENCES

1. Maydew, R. C., Peterson, C. W., and Orlik-Ruckemann, K. J., "Design and Testing of High-Performance Parachutes," AGARDograph No. 319, November 1991.
2. Cockrell, D. J., "The Aerodynamics of Parachutes," AGARDograph No. 295, July 1987.
3. Knacke, T. W., "Parachute Recovery Systems Design Manual," NWCTP 6575, Naval Weapons Center, China Lake, California, June 1987.
4. Ewing, E. G., Bixby, H. W., and Knacke, T. W., "Recovery Systems Design Guide," AFFDL-TR-78-151, December 1978.
5. Performance of and Design Criteria for Deployable Aerodynamic Decelerators, USAF ASD-TR-61-597, December 1963.
6. AIAA 1<sup>st</sup> Aerodynamic Deceleration Systems Conference, Houston, Texas, September 1966.
7. Klimas, P. C., "Internal Parachute Flows," Journal of Aircraft, Vol. 9, No. 4, April 1972.
8. Rogers, S. E., Kwak, D., and Kiris, C., "Steady and Unsteady Solutions of the Incompressible Navier-Stokes Equations," AIAA Journal, Vol. 29, No. 4, pp. 603-610, April 1991
9. Rogers, S. E., Wiltberger, N. L., and Kwak, D., "Efficient Simulation of Incompressible Viscous Flow over Single and Multielement Airfoils," Journal of Aircraft, Vol. 30, No. 5, pp. 736-743, September-October 1993.
10. Kwak, D., "Computation of Viscous Incompressible Flows," NASA Technical Memorandum 101090, March 1989.
11. Baldwin, B. S. and Barth, T. J., "A One-Equation Turbulence Transport Model for High Reynolds Number Wall-Bounded Flows," AIAA Paper No. 91-0610, 1991.
12. Sundberg, W. D., "New Solution Method for Steady-State Canopy Structural Loads," Journal of Aircraft, Vol. 25, No. 11., November 1988.
13. Benney, R. J., and Leonard, J., "A 3-D Finite Element Structural Parachute Model," Paper No. 95-1563 13<sup>th</sup> AIAA Aerodynamic Decelerator Conference May 1995.
14. Stein, K. R., and Benney, R. J., "Parachute Inflation: A Problem in Aeroelasticity," U.S. Army Natick Research, Development, and Engineering Center. Natick Technical Report No. NATICK/TR-94/015, August 1994.
15. Thompson, J., "A Composite Grid Generation Code for 3-D Region - The EAGLE Code," AIAA Journal, Vol. 26, No. 3, pp. 271-272, March 1988.

INTENTIONALLY LEFT BLANK

<u>NO. OF COPIES</u>	<u>ORGANIZATION</u>	<u>NO. OF COPIES</u>	<u>ORGANIZATION</u>
2	ADMINISTRATOR DEFENSE TECHNICAL INFO CENTER ATTN DTIC DDA 8725 JOHN J KINGMAN RD STE 0944 FT BELVOIR VA 22060-6218	2	ARPA ATTN DR P KEMMEY DR JAMES RICHARDSON 3701 NORTH FAIRFAX DR ARLINGTON VA 22203-1714
1	DIRECTOR US ARMY RESEARCH LABORATORY ATTN AMSRL CS AL TA RECORDS MANAGEMENT 2800 POWDER MILL RD ADELPHI MD 20783-1197	7	DIRECTOR NASA AMES RESEARCH CENTER ATTN MS 227 8 L SCHIFF MS 258 1 T HOLST MS 258 1 D CHAUSSEE MS 258 1 M RAI MS 258 1 P KUTLER MS 258 1 P BUNING MS 258 1 B MEAKIN MOFFETT FIELD CA 94035
1	DIRECTOR US ARMY RESEARCH LABORATORY ATTN AMSRL CI LL TECHNICAL LIBRARY 2800 POWDER MILL RD ADELPHI MD 207830-1197	2	USMA DEPT OF MECHANICS ATTN LTC ANDREW L DULL M COSTELLO WEST POINT NY 10996
1	DIRECTOR US ARMY RESEARCH LABORATORY ATTN AMSRL CS AL TP TECH PUBLISHING BRANCH 2800 POWDER MILL RD ADELPHI MD 20783-1197	7	COMMANDER US ARMY ARDEC ATTN MCAR AET A R DEKLEINE C NG R BOTTICELLI H HUDGINS J GRAU S KAHN W KOENIG PICATINNY ARSENAL NJ 07806-5001
2	USAF WRIGHT AERONAUTICAL LABORATORIES ATTN AFWAL FIMG DR J SHANG MR N E SCAGGS WPAFB OH 45433-6553	1	COMMANDER US ARMY ARDEC ATTN SMCAR CCH V PAUL VALENTI PICATINNY ARSENAL NJ 07806-5001
1	COMMANDER NAVAL SURFACE WARFARE CNTR ATTN CODE B40 DR W YANTA DAHLGREN VA 22448-5100	1	COMMANDER US ARMY ARDEC ATTN SFAE FAS SD MIKE DEVINE PICATINNY ARSENAL NJ 07806-5001
1	COMMANDER NAVAL SURFACE WARFARE CNTR ATTN CODE 420 DR A WARDLAW INDIAN HEAD MD 20640-5035	1	COMMANDER US NAVAL SURFACE WEAPONS CTR ATTN DR F MOORE DAHLGREN VA 22448
4	DIRECTOR NASA LANGLEY RESEARCH CENTER ATTN TECH LIBRARY MR D M BUSHNELL DR M J HEMSCH DR J SOUTH LANGLEY STATION HAMPTON VA 23665	2	UNIV OF CALIFORNIA DAVIS DEPT OF MECHANICAL ENGG ATTN PROF H A DWYER PROF M HAFEZ DAVIS CA 95616

<u>NO. OF COPIES</u>	<u>ORGANIZATION</u>	<u>NO. OF COPIES</u>	<u>ORGANIZATION</u>
1	AEROJET ELECTRONICS PLANT ATTN DANIEL W PILLASCH B170 DEPT 5311 P O BOX 296 1100 WEST HOLLYVALE STREET AZUSA CA 91702	1	NAVAL AIR WARFARE CENTER ATTN DAVID FINDLAY MS 3 BLDG 2187 PATUXENT RIVER MD 20670
3	SCIENCE AND TECHNOLOGY INC 4001 NORTH FAIRFAX DR NO 700 ATTN DR ALAN GLASSER MR BRUCE LOHMAN MR DAVE MAURIZI ARLINGTON VA 22203-1618	1	METACOMP TECHNOLOGIES INC ATTN S R CHAKRAVARTHY 650 S WESTLAKE BLVD SUITE 200 WESTLAKE VILLAGE CA 91362-3804
3	AIR FORCE ARMAMENT LAB ATTN AFATL/FXA STEPHEN C KORN BRUCE SIMPSON DAVE BELK EGLIN AFB FL 32542-5434	2	ROCKWELL SCIENCE CENTER ATTN S V RAMAKRISHNAN V V SHANKAR 1049 CAMINO DOS RIOS THOUSAND OAKS CA 91360
1	MASSACHUSETTS INSTITUTE OF TECHNOLOGY ATTN TECH LIBRARY 77 MASSACHUSETTS AVE CAMBRIDGE MA 02139	1	ADVANCED TECHNOLOGY CTR ARVIN/CALSPAN AERODYNAMICS RESEARCH DEPT ATTN DR M S HOLDEN PO BOX 400 BUFFALO NY 14225
1	GRUMANN AEROSPACE CORP AEROPHYSICS RESEARCH DEPT ATTN DR R E MELNIK BETHPAGE NY 11714	1	PENNSYLVANIA STATE UNIV DEPT OF AEROSPACE ENGG ATTN DR G S DULIKRAVICH UNIVERSITY PARK PA 16802
2	MICRO CRAFT INC ATTN DR JOHN BENEK NORMAN SUHS 207 BIG SPRINGS AVE TULLAHOMA TN 37388-0370	1	UNIV OF ILLINOIS AT URBANA CHAMPAIGN DEPT OF MECHANICAL AND INDUSTRIAL ENGINEERING ATTN DR J C DUTTON URBANA IL 61801
1	LOS ALAMOS NATIONAL LAB ATTN MR BILL HOGAN MS G770 LOS ALAMOS NM 87545	1	UNIVERSITY OF MARYLAND DEPT OF AEROSPACE ENGG ATTN DR J D ANDERSON JR COLLEGE PARK MD 20742
3	DIRECTOR SANDIA NATIONAL LABORATORIES ATTN DIV 1554 DR W OBERKAMPF DIV 1554 DR F BLOTTNER DIV 1636 DR W WOLFE ALBUQUERQUE NM 87185	1	UNIVERSITY OF NOTRE DAME DEPT OF AERONAUTICAL AND MECHANICAL ENGINEERING ATTN PROF T J MUELLER NOTRE DAME IN 46556

<u>NO. OF COPIES</u>	<u>ORGANIZATION</u>	<u>NO. OF COPIES</u>	<u>ORGANIZATION</u>
1	UNIVERSITY OF TEXAS DEPT OF AEROSPACE ENG MECH ATTN DR D S DOLLING AUSTIN TX 78712-1055	2	CDR ARDEC ATTN FIRING TABLES R LIESKE R EITMILLER BLDG 120
1	UNIVERSITY OF DELAWARE DEPT OF MECH ENGINEERING ATTN DR JOHN MEAKIN NEWARK DE 19716		
1	UNIVERSITY OF FLORIDA DEPT OF ENGG SCIENCES COLLEGE OF ENGINEERING ATTN PROF C C HSU GAINESVILLE FL 32611		
3	COMMANDER US ARMY SOLDIER SYSTEMS CMD NRDEC ATTN SSCM UTS R BENNEY K STEIN C LEE NATICK MA 01760-5017		
<u>ABERDEEN PROVING GROUND</u>			
2	DIRECTOR US ARMY RESEARCH LABORATORY ATTN AMSRL CI LP (TECH LIB) BLDG 305 APG AA		
26	DIR USARL ATTN AMSRL WM P A HORST E SCHMIDT AMSRL WM PB P PLOSTINS D LYON M BUNDY G COOPER E FERRY B GUIDOS K HEAVEY H EDGE V OSKAY A MIKHAIL J SAHU P WEINACHT AMSRL ST J ROCCHIO AMSRL WM PD B BURNS AMSRL WM PA G KELLER M NUSCA AMSRL WM PC B FORCH AMSRL WM W C MURPHY AMSRL WM WB W D'AMICO AMSRL CI H C NIETUBICZ AMSRL CI HC P COLLINS D HISLEY D PRESSEL W STUREK		

INTENTIONALLY LEFT BLANK

# REPORT DOCUMENTATION PAGE

*Form Approved  
OMB No. 0704-0188*

Public reporting burden for this collection of information is estimated to average 1 hour per response, including the time for reviewing instructions, searching existing data sources, gathering and maintaining the data needed, and completing and reviewing the collection of information. Send comments regarding this burden estimate or any other aspect of this collection of information, including suggestions for reducing this burden, to Washington Headquarters Services, Directorate for Information Operations and Reports, 1215 Jefferson Davis Highway, Suite 1204, Arlington, VA 22202-4302, and to the Office of Management and Budget, Paperwork Reduction Project (0704-0188), Washington, DC 20503.

1. AGENCY USE ONLY <i>(Leave blank)</i>			2. REPORT DATE September 1997		3. REPORT TYPE AND DATES COVERED Final	
4. TITLE AND SUBTITLE  3-D Parachute Descent Analysis Using Coupled Computational Fluid Dynamic and Structural Codes					5. FUNDING NUMBERS  PR: 1L161102AH43	
6. AUTHOR(S)  Sahu, J.; Cooper, G. R. (ARL); Benney, R.J. (U.S. Army Soldier Systems Command)						
7. PERFORMING ORGANIZATION NAME(S) AND ADDRESS(ES)  U.S. Army Research Laboratory Weapons & Materials Research Directorate Aberdeen Proving Ground, MD 21010-5066					8. PERFORMING ORGANIZATION REPORT NUMBER	
9. SPONSORING/MONITORING AGENCY NAME(S) AND ADDRESS(ES)  U.S. Army Research Laboratory Weapons & Materials Research Directorate Aberdeen Proving Ground, MD 21010-5066					10. SPONSORING/MONITORING AGENCY REPORT NUMBER  ARL-TR-1435	
11. SUPPLEMENTARY NOTES						
12a. DISTRIBUTION/AVAILABILITY STATEMENT  Approved for public release; distribution is unlimited.				12b. DISTRIBUTION CODE		
13. ABSTRACT <i>(Maximum 200 words)</i>  A computational tool that models the terminal descent characteristics of a single or a cluster of parachutes is a technology that is needed by parachute designers and engineers. As part of a technology program annex (TPA), a joint effort between the U.S. Army Natick Research, Development, and Engineering Center (NRDEC) and the U.S. Army Research Laboratory (ARL) to develop this computational tool is now under way. As a first effort, attempts are being made to analyze both two-dimensional (2-D) and three-dimensional (3-D) flow fields around a parachute using a coupling procedure in which the fluid dynamics are coupled to 2-D and 3-D structural dynamic (SD) codes. This effort uses computational fluid dynamic (CFD) codes to calculate a pressure field, which is then used as an input load for the SD code. Specifically, this report presents the methods and results of the flow field plus the structural characteristics of a single axisymmetric parachute and a 3-D gore configuration for the terminal descent velocity. Computed results have been obtained using the payload weight and unstretched constructed geometry of the canopies as input. Significant progress has been made in determining the terminal descent flow field along with the terminal shape of the parachute. A discussion of the fluid and structural dynamics codes, coupling procedure, and the associated technical difficulties is presented. Examples of the codes' current capabilities are shown.						
14. SUBJECT TERMS  fluids-structures compiling incompressible flow low speed flow				Navier-Stokes solution parachutes terminal descent		15. NUMBER OF PAGES 33
						16. PRICE CODE
17. SECURITY CLASSIFICATION OF REPORT Unclassified		18. SECURITY CLASSIFICATION OF THIS PAGE Unclassified		19. SECURITY CLASSIFICATION OF ABSTRACT Unclassified		20. LIMITATION OF ABSTRACT